Femtosecond ytterbium fiber laser with photonic crystal fiber for dispersion control

H. Lim, F. Ö. Ilday, and F. W. Wise

Department of Applied Physics, Cornell University, Ithaca, New York 14853

hl247@cornell.edu

Abstract: We demonstrate the use of photonic-crystal fiber for dispersion compensation in a soliton fiber laser. The anomalous dispersion provided by the photonic-crystal fiber enables us to construct a femtosecond fiber laser at 1 μm wavelength without prisms or diffraction gratings. The laser produces ~100-fs pulses with 1 nJ energy, and is a major step toward environmentally-stable all-fiber devices at 1 μm.

© 2002 Optical Society of America

OCIS codes: (140.3510) Lasers, fiber; (320.7090) Ultrafast lasers

References and links

1. H. A. Haus, J. G. Fujimoto, and E. P. Ippen, "Analytic theory of additive pulse and Kerr lens mode locking," IEEE J. Quantum Electron. **28**, 2086-2096 (1992).
2. T. Brabec, Ch. Spielmann, and F. Krausz, "Mode locking in solitary lasers," Opt. Lett. **16**, 1961-1963 (1991).
3. I. N. Duling, III, "Subpicosecond all-fiber erbium laser," Electron. Lett. **27**, 544-545 (1991).
4. K. Tamura, E. P. Ippen, H. A. Haus, and L. E. Nelson, "77-fs pulse generation from a stretched-pulse mode-locked all-fiber ring laser," Opt. Lett. **18**, 1080-1082 (1993).
5. H. Lim, F. Ö. Ilday, and F. W. Wise, "Generation of 2-nJ pulses from a femtosecond Yb fiber laser," accepted for publication in Opt. Lett.
6. V. Cautaerts, D. J. Richardson, R. Paschotta, and D. C. Hanna, "Stretched pulse Yb^{3+}-silica fiber laser," Opt. Lett. **22**, 316-318 (1997).
7. L. Lefort, J. H. V. Price, D. J. Richardson, G. J. Spühler, R. Paschotta, U. Keller, A. R. Fry, and J. Weston, "Practical low-noise stretched-pulse Yb^{3+}-doped fiber laser," Opt. Lett. **27**, 291-293 (2002).
8. J. Limpert, A. Liem, T. Gabler, H. Zellmer, A. Tünermann, S. Unger, S. Jetschke, and H. -R. Müller, "High-average-power picosecond Yb-doped fiber amplifier," Opt. Lett. **26**, 1849-1851 (2001).
9. M. E. Fermann, A. Galvanauskas, M. L. Stock, K. K. Wong, and D. Harter, "Ultrawide tunable Er soliton fiber laser amplified in Yb-doped fiber," Opt. Lett. **24**, 1428-1430 (1999).
10. J. C. Knight, T. A. Birks, P. St. J. Russel, and D. M. Atkin, "All-silica single-mode fibr with photonic crystal cladding", Opt. Lett. **21**, 1547-1549 (1996).
11. D. Mogilevtsev, T. A. Birks, and P. St.J. Russell, "Group-velocity dispersion in photonic crystal fibers," Opt. Lett. **23**, 1662-1664 (1998).
12. K. Furusawa, T.M. Monro, P. Petropoulos, and D.J. Richardson, "Modelocked laser based on ytterbium doped holey fibre", Electron. Lett. **37**, 560-561 (2001).
13. S. M. J. Kelly, "Characteristic sideband instability of periodically amplified average soliton," Electron. Lett. **28**, 806-807 (1992).
14. W. J. Wadsworth, J. C. Knight, W. H. Reeves, P. S. J. Russell, and J. Arriaga, "Yb^{3+}-doped photonic crystal fibre laser," Electron. Lett. **36**, 1452-1453 (2000).

1. Introduction

Short-pulse fiber lasers offer a number of practical advantages over bulk solid-state lasers, including compact size and freedom from misalignment. These attributes derive

Received November 11, 2002; Revised December 09, 2002

from the availability of fiber with anomalous group-velocity dispersion (GVD); considering the usual soliton-like pulse formation in femtosecond modelocked lasers, anomalous GVD is needed to balance the positive Kerr nonlinearity of the fiber [1], [2]. Femtosecond erbium-doped fiber lasers at 1.55 μm can be constructed entirely of anomalous-GVD fiber to operate in the soliton regime [3], or with segments of normal-GVD and anomalous-GVD fiber to operate in the stretched-pulse regime [4].

There is great interest in the development of short-pulse fiber lasers at wavelengths below 1.3 μm, the zero-dispersion wavelength of standard silica fiber. However, efforts in this direction are hampered by the lack of anomalous-GVD fiber. Lasers must be constructed with bulk optical elements, which negates some of the major advantages of fiber. In particular, ytterbium-doped fiber is attractive for high-energy, short-pulse operation. Pulses as short as 50 fs and pulse energies as large as 2 nJ can be generated with Yb fiber [5], but all short-pulse Yb fiber lasers reported to date have employed prisms or diffraction gratings for anomalous GVD [5], [6], [7]. Yb-doped amplifiers provide the highest pulse energies and average powers available from fiber-based sources, but these are all seeded by bulk oscillators [8] or complicated multi-stage fiber sources with nonlinear wavelength conversions [9]. For greatest utility it would be highly desirable to seed these amplifiers with an integrated fiber source.

Photonic crystal fiber (PCF) is silica fiber with an ordered array of air holes along its length [10]. The novel properties of PCF include the possibility of anomalous GVD at wavelengths between 0.7 and 1.3 μm, determined primarily by the air filling fraction and thus effective core diameter [11]. PCF therefore offers a route to the construction of soliton fiber lasers at wavelengths below 1.3 μm. An actively modelocked ytterbium-doped PCF laser was reported [12]. However, the PCF had no influence in pulse shaping, other than providing gain.

Here we describe the first soliton fiber laser to exploit PCF for dispersion control. We demonstrate a Yb fiber laser comprised of segments of normal-GVD gain fiber and anomalous-GVD PCF. The laser generates positively-chirped pulses with 1 nJ energy, which are compressed to $\sim$100 fs with a grating pair external to the cavity. Optimization of this initial device for improved performance and environmental stability will be discussed.

2. Experimental

A Yb fiber laser with a PCF for dispersion control is conceptually the 1-μm analog of existing Er fiber lasers at 1.55 μm. Dispersive and nonlinear effects dominate the dynamics of pulsed operation in the femtosecond domain. Our choice of cavity parameters was guided by consideration of prior Er and Yb fiber lasers, and refined by numerical simulations of modelocking. Several issues arise in the use of PCF in soliton fiber laser. In contrast to a laser with prisms or diffraction gratings, a laser with a PCF can experience strong nonlinear effects in the anomalous-GVD segment of the cavity. Increased nonlinearity is desirable as a facilitator of modelocking. On the other hand, strong nonlinearity, particularly in combination with anomalous GVD, will degrade the pulse quality and limit the maximum pulse energy. A practical issue is that all PCF with small core size is highly birefringent (the beat length is a few mm). This property of PCF will eventually be exploited in the construction of environmentally-stable lasers. However, it is not compatible with the use of nonlinear polarization evolution (NPE) as an effective saturable absorber.

Considering these issues, we constructed the laser shown in Fig. 1. A unidirectional ring cavity is employed, to assist the initiation of mode-locking. The cavity allows NPE to occur and also has a segment where linear polarization is nominally maintained. We chose a PCF (2-μm core, 1.4-μm pitch and 0.7 average pitch-to-hole-size ratio, supplied

#1820 - $15.00 US Received November 11, 2002; Revised December 09, 2002
(C) 2002 OSA

by Crystal-Fibre A/S) to have substantial anomalous GVD (-40 ps^2/km) at 1 μm. The PCF is placed in a segment of the cavity where the polarization is linear. An in-line polarization controller converts the polarization to elliptical for NPE. We use a highly-doped Yb fiber (NA = 0.12, core diameter 6 μm, 23,600 ppm doping), which is 20 cm long. The Yb fiber is pumped at 980 nm by a laser diode capable of supplying up to 550 mW into single-mode fiber via a wavelength division multiplexed (WDM) coupler. The normal GVD of the gain fiber and leads is compensated by 1.3 m of PCF, which results in net anomalous GVD of 0.02 ps^2. With its relatively short fiber lengths and net anomalous dispersion, the laser is designed to operate in the weakly-stretched soliton regime. The output is taken directly from the NPE ejection port, which reduces the pulse energy in the PCF and linearly polarizes the field coupled into the PCF.

Even with a half-wave plate immediately before the PCF, there will be some residual excitation of the polarization mode orthogonal to the desired mode. In the time domain, the components of a pulse in the different modes walk off due to birefringence. Therefore, we expect that excitation of the undesired polarization mode may be a significant impediment to self-starting operation. A simplified model of the laser cavity was constructed to investigate the effect of birefringence on pulse start-up. Propagation in the fiber segments is described by the nonlinear Schrodinger equation that includes saturating, finite-bandwidth gain for the Yb fiber. Following the PCF, the field is split into two components corresponding to the different polarization modes. One of these is temporally delayed by a discrete amount corresponding to the fiber beat length, and the components are added together: $E(t)(1-\kappa)+E(t+\tau)\kappa$, where $E(t)$ is the optical field, κ is the coupling coefficient into the undesired mode, and τ is the delay. Numerical simulations of this model show that for a given pulse energy, the time required for modelocking to develop is linearly proportional to κ below a threshold value. For stronger coupling, stable modelocking cannot be obtained unless the pulse energy is increased.

Experimentally, the laser is not self-starting. Although this is not surprising, the crude nature of the model prevents us from concluding decisively that the birefringence prevents start-up; other effects could be involved and more work is needed to resolve this issue. With an acousto-optic mode-locker (AOM) in the cavity, modelocking is established easily by adjustment of the polarization controllers. Once initiated, the AOM is turned off and modelocking sustains itself, typically for hours. The pulse train is shown in Fig. 2. (All of the data presented in this paper were recorded with the AOM turned off.) With a repetition rate of 60 MHz, the pulse energy is 1 nJ.

The pulse autocorrelation is shown on several time-delay scales in Fig. 3, and the power spectrum is shown in Fig. 4. The long-range autocorrelation (Fig. 3 (a)) demonstrates single-soliton operation. The spectral sidebands (marked with arrows in Fig. 4) provide a signature of the soliton regime [13], and the GVD (-0.02 ps^2) inferred from the positions of the spectral sidebands agrees with the nominal cavity GVD. The interferometric autocorrelation of the compressed pulses is shown in Fig. 3 (c) along with the envelopes calculated from the measured power spectrum assuming that the phase is constant across the spectrum. The transform-limited pulse duration would be 80 fs. The experimental autocorrelation is 30% broader than the transform-limited version, so we cannot determine the pulse duration precisely. However, it is reasonable to conclude that the pulse duration is in the range 100 - 120 fs. Directly out of the laser, we measure the pulse duration to be 300 fs, which implies the stretching ratio is approximately 3. The birefringence of the PCF produces the deep modulation on the spectrum with a period of 2 nm, corresponding to 2-ps walk-off. The small secondary pulse located 2 ps from the main pulse (Fig. 3 (b)) originates in the component of the field in the undesired polarization mode of the PCF. This was independently verified by transmitting low-energy pulses through the PCF. The zero-phase Fourier transform of the modelocked spectrum

#1820 - $15.00 US Received November 11, 2002; Revised December 09, 2002
(C) 2002 OSA

produces a secondary pulse at the same 2-ps interval, and comparison with the cw lasing spectrum (also shown in Fig. 4 (b)) separately confirms that the spectral modulation and temporal location of the secondary pulse are consequences of the birefringence of the PCF. The secondary pulse contains 7% of the energy of the main pulse.

We emphasize that the origin of the secondary pulse is linear birefringence, to distinguish from the multiple-pulsing that occurs in modelocked lasers when the pulse energy is excessive. When the pump power is increased, multiple-pulsing (most commonly double-pulsing) is observed. The pulses are separated by tens of picoseconds, with the exact separation depending on the intracavity pulse energy. Each soliton is accompanied by the small secondary pulse seen in single-soliton operation, at the same fixed separation.

The performance of this initial laser can be improved substantially, and this will be addressed in future versions. With better polarization-mode suppression and/or increased passive amplitude modulation, self-starting operation should be possible. In addition, it is evident from numerical simulations that stronger pulse-stretching should be implemented for maximum pulse energy and minimum duration. Several nanojoules will apparently be possible, which would match the largest pulse energy produced by a fiber laser, and be comparable to the pulse energy of a Ti:sapphire laser. Finally, an environmentally-stable soliton laser could be made with polarization-maintaining gain fiber or from a single piece of PCF doped with active ions [14].

3. Conclusion

We have demonstrated a 1-μm soliton laser with dispersion controlled by a PCF. The performance and practical advantages of all-fiber lasers at 1.55 μm are available at 1 μm as a result of this work, and extensions to other wavelengths between 0.7 and 1.3 μm will follow as gain media are developed. We expect that the resulting stable, all-fiber devices will find numerous applications.

4. Acknowledgement

This work was supported by the National Institutes of Health under grant RR10075, the National Science Foundation, and Clark/MXR, Inc.. The authors thank Coherent, Inc. for providing a high-power laser diode.

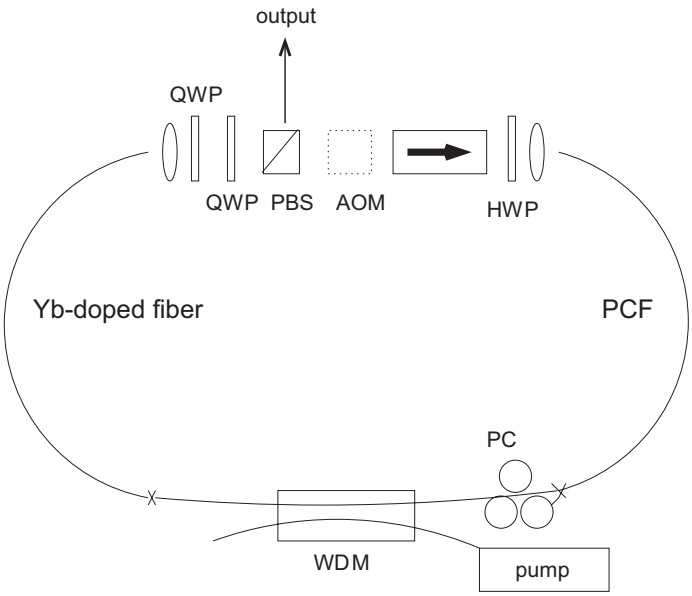

Fig. 1. Schematic of the laser. QWP: quarter-wave plate; HWP: half-wave plate; PBS: polarizing beam splitter; PC: polarization controller.

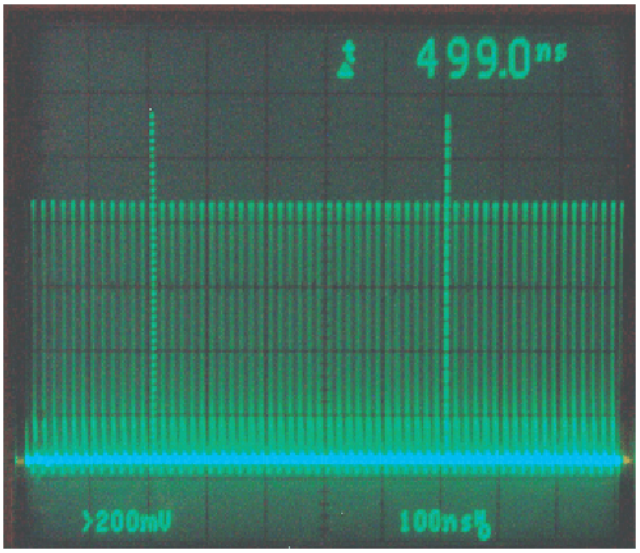

Fig. 2. Pulse train.

#1820 - $15.00 US
Received November 11, 2002; Revised December 09, 2002
(C) 2002 OSA

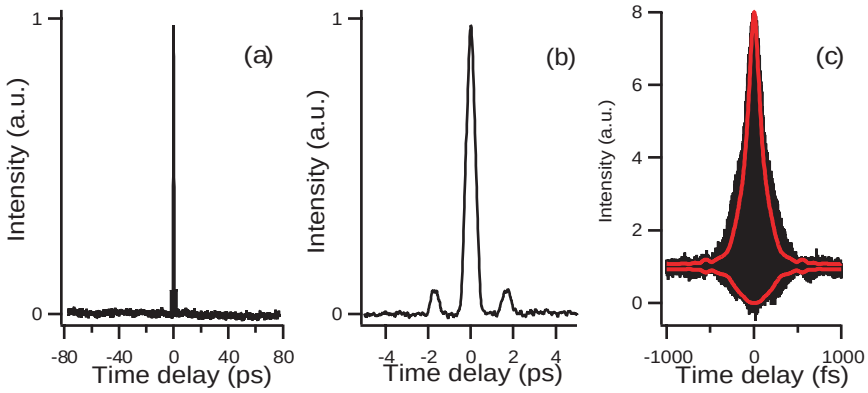

Fig. 3. Autocorrelation of the pulses from the Yb fiber laser, recorded over the indicated ranges of delay. (c) Measured interferometric autocorrelation (black) and envelopes calculated from the measured power spectrum (red).

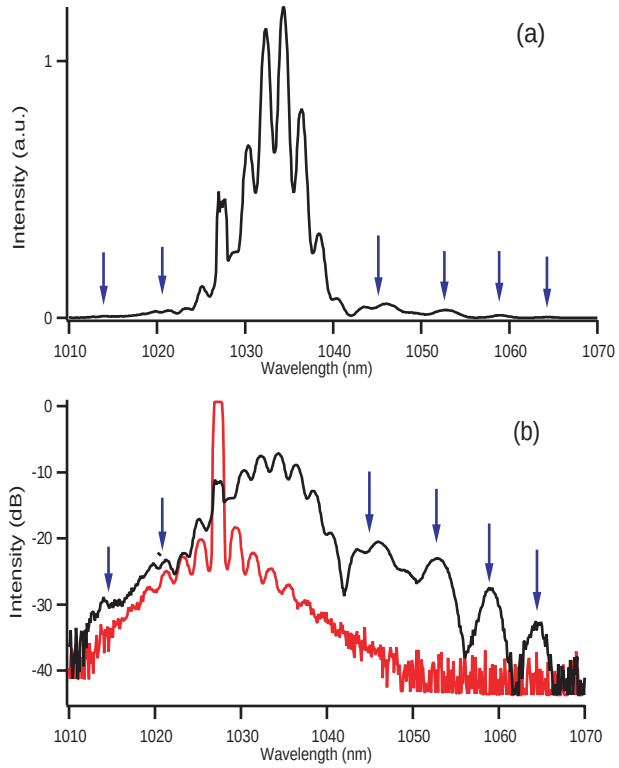

Fig. 4. Spectrum on (a) linear and (b) logarithmic scales. Spectral sidebands are marked with arrows. The cw lasing spectrum of the laser (red line in (b)) is also shown for comparison.

#1820 - $15.00 US
Received November 11, 2002; Revised December 09, 2002
(C) 2002 OSA